Microstructural characterization of hydroxyapatite-alendronate nanocomposites

D. NEGREA, C. DUCU, S. MOGA, V. MALINOVSCHI, J. NEAMTU[a],
C. RISTOSCU[b], I. N. MIHAILESCU[b*], F. CORNELIA[a]
University of Pitesti – Research Centre for Advanced Materials, Romania
[a]*University of Medicine and Pharmacy of Craiova, Romania*
[b]*National Institute for Lasers, Plasma and Radiation Physics, Lasers Department, Magurele-Ilfov, Romania*

Hydroxyapatite (HA) is an important bioactive material, quite appropriate for repairing or replacing bone tissues due to its resemblance to mineral components of bone and teeth. Bisphosphonates (BPs), e.g. alendronate (AL), are a class of compounds widely used for the treatment of disorders of bone metabolism. The synthesis of nanocrystalline HA containing alendronate opens a new way to the application of these composite biomaterials for hard tissue cure and repair. It is therefore important to evaluate the microstructural changes that might be induced by the synthesis process of HA-AL. We analyzed synthesized HA-AL composites with different BPs content of 3.9%wt to 7.1%wt to determine their microstructural properties. The composites were evaluated using powder X-ray Diffraction (XRD), Fourier Transform Infrared Spectroscopy (FTIR) and Scanning Electron Microscopy (SEM) combined with Energy Dispersive with Spectrometry (EDX). The obtained results revealed that alendronate is incorporated into HA crystals up to about 7.1%wt, without significantly affecting the lattice constants of HA. However, at 7.1%wt AL added, we noticed the characteristic crystalline phase of the composite. The Ca/P molar ratio was determined as a function of AL content. The results indicate no significant variation of the atomic positions, occupancy factors, and thermal parameters of hydroxyapatite. Alendronate affects nevertheless the size of the HA crystallites which exhibit significantly smaller dimensions when increasing AL concentration.

1. Introduction

Hydroxylapatite, also called hydroxyapatite, is a naturally occurring mineral form of calcium apatite with the chemical formula $Ca_5(PO_4)_3(OH)$. It crystallizes in the hexagonal system. The OH^- ion can be replaced by fluoride, chloride or carbonate. Hydroxylapatite can be found in human teeth and bones. Thus, it is commonly used as a filler to replace amputated bone or as a coating to promote bone ingrowth into prosthetic implants. Microcrystalline hydroxyapatite (MH) is marketed as a "bone-building" supplement with superior absorption than calcium. Even many other phases exist with similar or even identical chemical makeup, the body responds much differently to them. Many modern implants, e.g. hip replacements and dental implants, are coated with hydroxyapatite due to the fact that it promotes the osseo-integration as the direct structural and functional connection between living bone and the surface of a load-bearing artificial implant, typically manufactured of titanium. It is a property virtually unique to titanium and hydroxylapatite, and has propulsed the science of medical bone, and joint replacement techniques.

Bisphosphonates (BPs) are a class of compounds widely used for the management of disorders of bone metabolism, such as Paget bone disease, osteoporosis, fibrous dysplasia, myeloma and bone metastases [1]. In particular, oral BPs have become the most widely used drugs in the treatment of osteoporosis; they significantly reduce the risk of new fractures in women with postmenopausal osteoporosis. BPs display a common backbone structure of P–C–P, where C is carbon and each P is a phosphonate group [2]. The two phosphonate groups are essential both for binding to hydroxyapatite (HA) and for the biochemical mechanism of action. Individual BPs are characterized by the two covalently bonded side chains attached to the central carbon atom, termed R1 and R2, which determine the efficiency of the compound. Binding to bone is enhanced when R1 is a hydroxyl group, whereas the R2 side group has some effect on binding but predominantly determines the antiresorptive potency of the BPs. In particular, the R2 side chain of nitrogen-containing BPs, N-BPs, can also influence overall bone affinity as a result of the ability of the nitrogen moiety to interact with the crystal surface of bone mineral [3-6].

Recently, an increasing body of literature has suggested that BP use, especially intravenous preparations, may be associated with osteonecrosis of the jaws. Thus, some experts caution that the benefits of prolonged use of BPs must be carefully weighed against the potential negative effects of over suppression of bone metabolism [7]. On this basis, the development of strategies for local administration of BPs becomes mandatory. The great attraction of BPs for calcium hinders the direct synthesis of HA crystals modified with BPs. That is why appropriate

approaches to synthesize HA–AL composite nanocrystals needs to be found.

Sodium alendronate is an aminobiphosphonate which binds to hydroxyapatite within bone structure and acts like a specific inhibitor of osteoclasts osseo-resorption.

In order to verify the projected properties of the obtained composite, a rigorous microstructural analysis has to be made.

2. Experimental

2.1 The synthesis of AL–HA nanocrystals

The synthesis of AL–HA nanocrystals was carried out using a recent method [2]. Briefly, 50 ml of 1.08 M $Ca(NO_3)_2 \times 4H_2O$ solution at pH adjusted to 10 with NH_4OH was heated at 90 ^oC in N_2 atmosphere and 50 ml of 0.65 M $(NH_4)HPO_4$ solution, pH 10 adjusted with NH_4OH, was added dropwise under stirring. Soon after completion of the phosphate addition, the AL solution was dropped under stirring in the reaction vessel. The precipitate was maintained in contact with the reaction solution for 5 h at 90 ^oC under stirring, then centrifuged at 10,000 rpm for 10 min and repeatedly washed with CO_2-free distilled water. The product was dried at 37 ^oC overnight. Using AL concentrations of 0, 7, and 28 mM (0, 3.9 and 7.1 wt%, respectively) two samples were prepared (HA–ALm, and HA–ALh).

2.2 Methods of investigation

SEM analysis of the HA-AL composites was performed using a FEI Inspect S scanning electron microscope. FTIR analysis was performed with a Nicolet iN10 Infrared Microscope. XRD analysis was performed on a Rigaku Ultima IV X-ray diffractometer in parallel set-up. In order to perform the Rietveld microstructural analysis and eliminate the instrumental contribution within the experimental diffraction pattern, a LaB_6 standard powder reference material was used.

3. Results and discussion

3.1 SEM analysis

The Ca/P molar ratio was determined as a function of AL content. It was noticed that Ca/P molar ratio (Ca/P = 1.67) is not significantly affected by alendronate incorporation.

3.2 FTIR analysis

Using the IR Nicolet iN10 microspectrophotometer it has been obtain the hydroxyapatite spectra together with the one of the composite HA-ALh (figure 1).
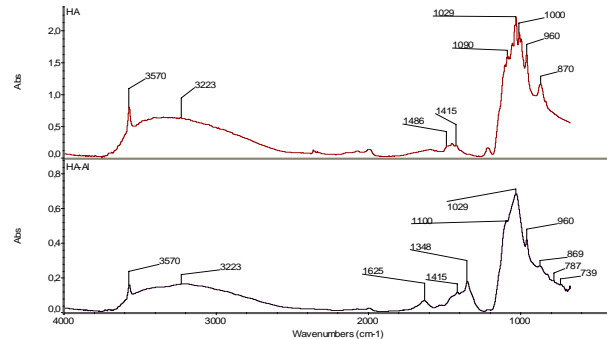

Fig. 1. Typical HA and HA-ALh FTIR spectra.

FTIR analysis of the samples spectra has revealed the following:

i. the peak associated to wave number of 3570 cm^{-1}, which can be observed in both cases, is due to the stretching mode of the O-H groups;

ii. the wide band around 3223 cm^{-1}, within the region corresponding to the stretching mode of the O-H groups associated by hydrogen bonds, is attributed to the absorbed water;

iii. the region from 1625 cm^{-1} that can be observed only on the composite HA-AL spectrum, can be attributed to the bending mode of NH_2 group as a prime amine compound. To the same group can also be attributed the 787 cm^{-1} peak observed only on the composite spectrum due to the wagging mode of the prime amine compound;

iv. the 1415 cm^{-1} and 1486 cm^{-1} peaks may be attributed to the carbonate ion CO_3^{2-}, present as impurity both in HA and composite. To the same ion can be attributed the 870 cm^{-1} and 869 cm^{-1} peaks;

v. the 1348 cm^{-1} peak may be attributed to the bending mode of the O-H group;

vi. within the region of 800-1100 cm^{-1} we noticed a series of peaks that are characteristic to the phosphate ion oscillation modes. Although they can be observed in both spectra, their presence is characteristic especially to crystalline HA. Because in HA spectrum, these peaks are outnumber and sharper than composite, it follows that HA is more crystalline that the HA-AL compound;

vii. the 739 cm^{-1} peak, that can be observed only in the composite spectrum, can be attributed to the rocking mode of methylene groups (CH_2).

3.3 XRD analysis

XRD analysis was performed on a Rigaku Ultima IV X-ray diffractometer in parallel set-up for higher resolution, using Cu K_α radiation obtained at U=40 kV and I=30 mA, 0.02^o angular step and 15 sec/step. In order to perform the Rietveld microstructural analysis and eliminate the instrumental contribution within the experimental diffraction pattern, a LaB_6 standard powder reference material (fig. 2) was used. [8]
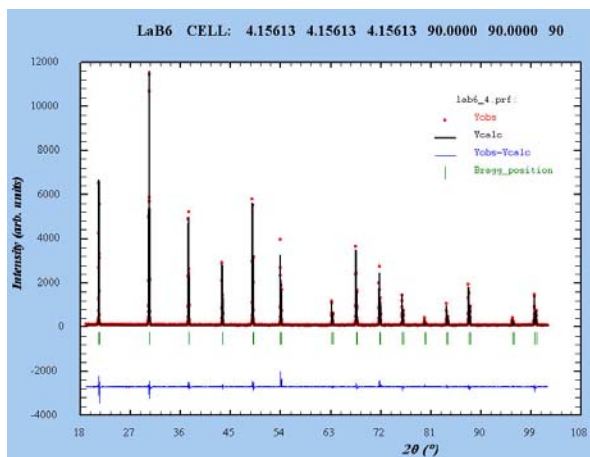
Fig. 2. XRD pattern for LaB$_6$ standard powder reference material.

The Gaussian and Lorentzian components of the LaB$_6$ peak profiles have been drawn and instrumental resolution file was written.

The microstructural effects are treated using the Voigt approximation: both instrumental and sample intrinsic profiles were supposed to be described approximately by a convolution of Lorentzian and Gaussian components. The TCH pseudo-Voigt profile function is used to mimic the exact Voigt function [9,10].

Rietveld analysis was performed with the help of WinPLOTR [11] and FullProf [12] software (Fig. 3).
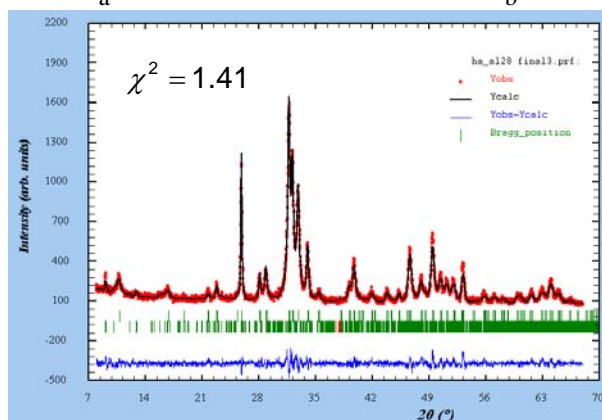
The integral breadth method to obtain volume averages of sizes and strains was used to output microstructural information which contains analysis of the size and strain contribution to each reflection (Table 1).
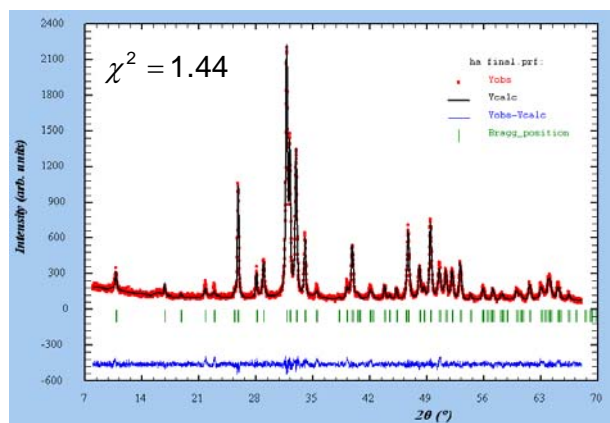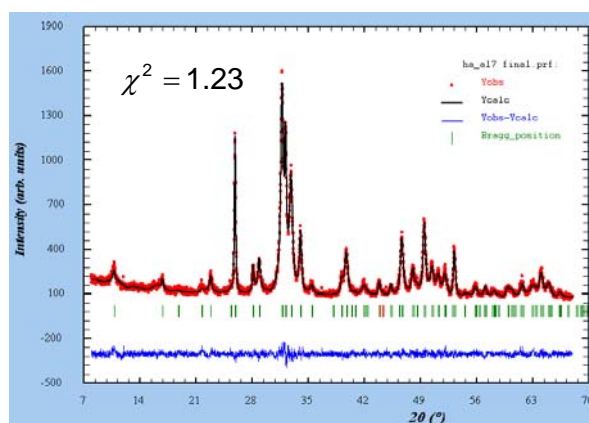
Fig. 3. Rietveld refinement for (a) HA, (b) HA-ALm and (c) HA-ALh samples

The standard deviation appearing in the global average apparent size and strain was calculated using the different reciprocal lattice directions. It stands a measure of the degree of anisotropy, not of the estimated error.

A phenomenological treatment of line broadening in terms of coherent domain size and strains due to structural defects could also be drawn. [13]

Table 1. Microstructural data on size and strain contribution of reflections.

Sample	Lattice constants			Average apparent size (Å)	Standard deviation (anisotropy)	Average maximum strain (%%)	Standard deviation (anisotropy)
	a (Å)	b (Å)	c (Å)				
HA	9.415	9.415	6.895	508	94.15	21.75	0.5997
HA-ALm	9.432	9.432	6.881	294	117.32	28.94	0.9411
HA-ALh	9.441	9.441	6.887	179	9.29	172.54	0.0385

As visible from Table 1, lattice constants *a* and *b* increase monotonous with AL content added, while lattice constant *c* has minor fluctuations in all three samples.

On the other hand, Rietveld analysis revealed that the average apparent size of crystallites is decreasing (figure 4) while the average maximum lattice strain is increasing (figure 5) with the alendonate content in the composite.
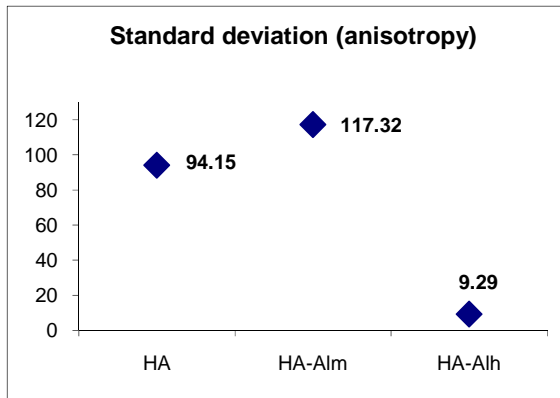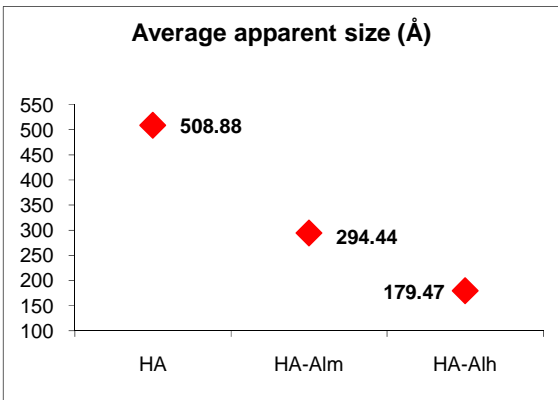

a

b

Fig. 4. Average apparent size (a)and anisotropy evolution (b)for the three samples analyzed .
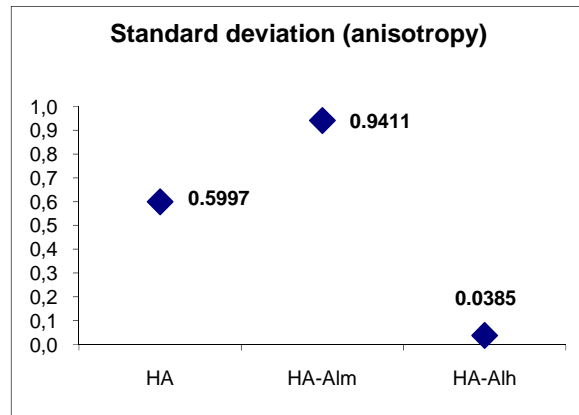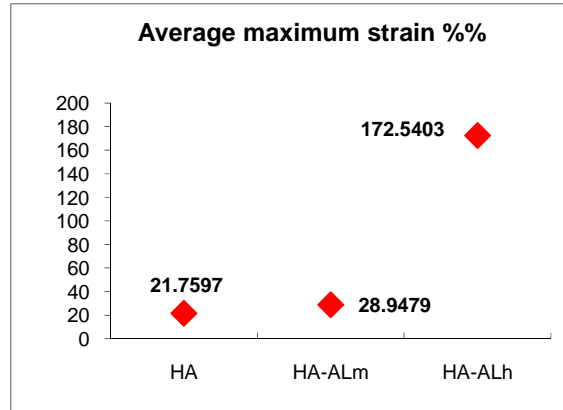

a

b

Fig. 5. Average maximum lattice strain (a) and anisotropy evolution (b) for the three samples analyzed

A detailed phase analysis has revealed that in the case of the composite HA-AL with 7.1 wt% alendronate, a characteristic crystalline phase of the composite (figure 6) appears.
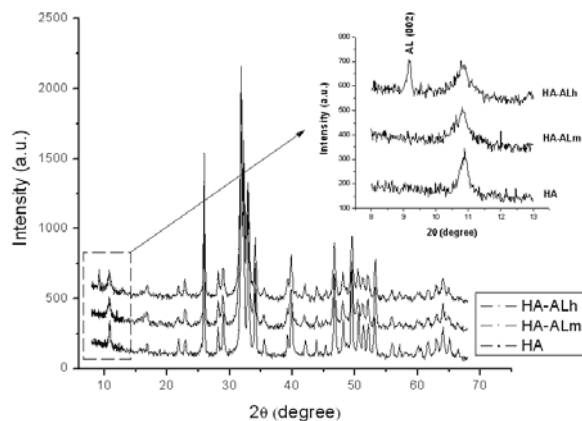
Fig. 6. HA, HA-ALm and HA-ALh diffraction spectra

When nanostructures are prepared by using chemical routes, some of the ions involved in the synthesis are frequently incorporated as impurities into the nanocrystals, expanding the lattice. This gives rise to changes in the macroscopic physical properties of the material, which can be well understood after a detailed atomic distribution analysis only. The samples in the initial crystallization step are usually a mixture of crystalline and amorphous phases. [14-17]
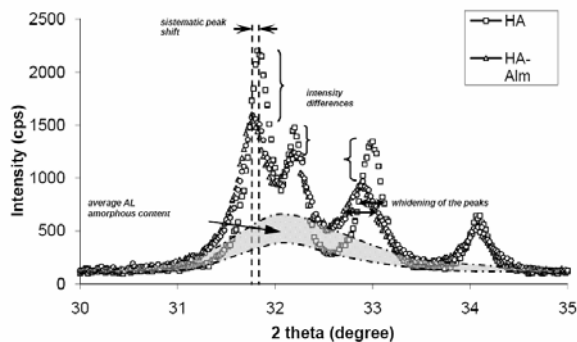

Fig. 7. HA, HA-ALm and HA-ALh diffraction spectra differences

X-ray diffraction peaks are broadened by small grain size and by lattice distortions caused by lattice defect. Accordingly, the diffracting domains are limited by the faults. As it can be noticed on the three spectra in figure 7, beside the AL amorphous content, there exists also peak profile differences due to the fact that AL atoms affects the HA crystalline lattice. This phenomenon could be explained by faulting theory. Various types of faults can be considered, e.g. deformation faults, growth faults, and twin faults. Stacking faults have three main effects on line profile: the apparent size is modified, the deformation faults introduce a shift of certain reflections in specific symmetries and asymmetry is observed in case of twinning [18].

4. Conclusions

Two types of composites powders based on HA synthesized with a different AL content of 3.9%wt and 7.1%wt were analyzed by XRD, FTIR and SEM.

The results revealed that alendronate is incorporated into HA crystals up to about 7.1%wt, without significantly affecting the lattice constants of the apatitic phase, as well the Ca/P molar ratio. On the other hand, the alendronate addition influences the HA crystallites, which exhibit significantly smaller sizes with increasing AL concentration. FTIR analysis has confirmed the incorporation of AL within the synthesized HA-AL composite and pointed out that HA is better crystallized that the HA-AL compound. Rietveld analysis has shown that the average maximum lattice strain is increasing with the alendonate content in composite. A detailed phase analysis has revealed that, in the case of HA-AL composite with AL concentration of 7.1 wt%, the alendronate compound exhibits its characteristic crystalline phase within the composite.

References

[1] H. Fleisch Bisphosphonates in bone disease, from the laboratory to the patient. San Diego: Academic Press; 2000.

[2] E. Boanini, M. Gazzano, K. Rubini, A. Bigi, Adv Mater; **19**, 2499 (2007).

[3] F. P. Coxon, K. Thompson, M. J. Rogers, Curr Opin Pharm **6**, 307 (2006).

[4] C. T. Leu, E. Luegmayr, L. P. Freedman, G. A. Rodan, A. A. Reszka, Bone **38**, 628 (2006).

[5] G. H. Nancollas, R. Tang, R. J. Phipps, Z. Henneman, S. Gulde, W. Wu, et al. Bone; **38,** 617 (2006).

[6] S. E. Papapoulos, Bone **38**, 613 (2006).

[7] H. Fleisch, Endocr Rev;**19,** 80 (1998).

[8] R. A. Young, "The Rietveld Method", Oxford University Press: New York (1993)

[9] Thompson, Cox and Hastings, J. Appl. Cryst. **20**, 79 (1987).

[10] X. Bokhimi, A. Morales, O. Novaro, T. Lopez, R. Gomez, A. Garcia-Ruiz, Quantitative analysis of phase transformation in nanocrystalline materials via Rietveld Refinement, JCPDS-International Centre for Diffraction Data 2000, Advances in X-ray Analysis, Vol.42.

[11] T. Roisnel, J. Rodriguez-Carvajal, Reference:WinPLOTR: a Windows tool for powder diffraction patterns analysis Materials Science Forum, Proceedings of the Seventh European Powder Diffraction Conference (EPDIC 7), 2000, p.118-123, Eds: R. Delhez and E.J. Mittenmeijer

[12] Juan Rodriguez-Carvajal, Thierry Roisnel, FullProf.98 and WinPLOTR: New Windows 95/NT Applications for Diffraction Commission For Powder Diffraction, International Union for Crystallography, Newletter N°20 (May-

August) Summer 1998

[13] X. Bokhimi, A. Morales, M. A. Lucatero, R. Ramírez, Nanostructured Materials **9**(1-8), 315 (1997).

[14] X. Bokhimi, A. Morales, T. Lopez, R. Gomez, J. Solid State Chem., **115,** 411 (1995).

[15] X. Bokhimi, A. Morales, O. Novaro, T. Lopez, E. Sanchez y, R. Gomez, J. Mater. Res, **10,** 2788 (1995).

[16] X. Bokhimi, A. Morales, O. Novaro, M. Portilla, T. Lopez, F. Tzompanzi, R. Gomez, J. Solid State Chem., **135,** 28 (1998).

[17] D. E. Newbury, Nanostructured Materials **9,** 251 (1995).

[18] D. Louer, N. Audebrand, Microstructure analysis of nanocrystalline powders by X-ray diffraction, **102** (2002) Acta Physica Polonica A No.1, Proceedings of the IV ISSP MS'01, Jaszowiec 2001.

_____

[*]Corresponding author: ion.mihailescu@inflpr.ro